JOURNAL OF COMPUTATIONAL PHYSICS 50, 337–359 (1983)

Quiet Starts for Galaxy Simulations*

J. A. SELLWOOD

Institute of Astronomy, Madingley Road, Cambridge CB3 OHA, England

Received February 2, 1982

The ability of computer simulations to reproduce the normal modes of disc galaxies is assessed. Two types of disc are studied: one in which all stars move initially on circular orbits and a second case in which stars have a broad distribution of initial velocities causing them individually to follow eccentric orbits. Quiet start procedures are developed and found to be advisable for both cases. The observed mode frequencies in the cold disc models are within 2% of the linear theory values while discrepancies of ~10% arise in the warm disc models. Nonquiet starts can lead to errors in excess of 50% when the same number of particles is used. The polar grid used for the simulations is shown to have further advantages over conventional Cartesian grids.

INTRODUCTION

The internal dynamics of a galaxy is that of a massive, collisionless (Vlasov) fluid which moves under the influence of its own self-gravity. Consequently, simulation techniques began as straightforward adaptations of the particle/mesh methods which had been successfully developed for plasmas [1, 2]. Despite their having made important contributions to our understanding of disc galaxies (a recent review may be found in [2]), there is still a worrying lack of information on the performance of galaxy codes. In particular, very few attempts have been made to check the models against the predictions of linear theory. There are two reasons for this, first, few linear results are available for comparison; second, the major interest in the simulations stems from the nonlinear behaviour they manifest. Yet such checks are important, since unless linear behaviour is correctly reproduced we must be sceptical of nonlinear results. Also quantitative comparison with linear results affords a much needed guide to the size of the calculation necessary for a particular purpose.

As for plasma simulation, the principal achievement of the codes is to approach the Vlasov limit whilst employing relatively few particles; typically 10^4–10^5 to represent a system of 10^{11}–10^{12} stars. Finite-size particles, introduced either explicitly, or implicitly through the spatial grid, are the key to this [7]. Replacing

* Work supported by an SERC post-doctoral fellowship.

0021-9991/83 $3.00

581/50/3-2

each point particle by a cloud may be viewed equally as smoothing the density distribution or softening the interparticle force.

Fluctuations, or noise, arising from the comparatively small number of particles, cause much higher amplitudes in all harmonics of the density spectrum than we expect in the real system. Finite-size particles smooth the short wavelength fluctuations which, as noted, would otherwise spoil the collisionless properties of the model [7]. The longer wavelength noise remains and is only slowly reduced by the "brute force" technique of employing ever larger numbers of particles.

Byers and Grewal [8], recognising this, showed that spacing particles evenly, rather than at random, could eliminate noise "completely." They measured the growth of an instability in a cold 1–D plasma simulation at "precisely" the rate predicted by linear theory. The idea has developed into the well-known quiet start procedure, and several authors [9–12] have demonstrated that it substantially improves the precision attainable from multidimensional, warm plasma simulations. The value of the technique has not previously been demonstrated for galaxy simulations.

Careful studies by several authors [3–5, 16] leave little room for doubt that qualitatively galaxy models behave correctly, but the only quantitative comparisons with linear theory are credited to Miller [23] who confined his attention to axisymmetric disturbances, and to Zang and Hohl [6]. Zang and Hohl obtained growth rates from their models between 10% and 30% lower than Kalnajs' (unpublished) theoretical values for the most unstable modes in a group of isochrone discs. They attributed the reduced growth rates in their models to the implicit softening of the mode potential introduced by their grid.

In this paper the growth of nonaxisymmetric modes in two types of unstable stellar disc is compared with the predictions of linear theory for each case. Section 3 contains description of models which reproduce the linear growth of the modes in a simple stellar disc, to a precision of 2%. The stars in this disc begin by moving on circular orbits so that the distribution function has zero width in velocity space and the disc is said to be cold. Kalnajs and Toomre (unpublished) utilised a softened gravitational potential when determining the modes, in order to suppress consequent local instabilities, so it is reassuring that computer models so closely mimic their predictions.

The models described in Section 4 are of warm, uniformly rotating discs whose modes were determined by Kalnajs [15]. Softening depresses the growth rates of unstable modes in the models, but the growth rates and pattern speeds of the modes measured from several experiments having varying degrees of softening extrapolate to within 10% of the theoretical values at zero softening.

Quiet start procedures are essential if this level of accuracy is to be obtained. Noisy starts, even with enormous numbers of particles, can give substantial errors in growth rates: over 50% in the worst cases. A method directly comparable to that used by Byers and Grewal [8] works very well for the cold discs and a logical extension of their method, not related to the moment correction method of Gitomer [10], is developed here for warm discs.

The computer code, described in Section 2, is designed specifically for simulations of disc galaxies. Its origins lie in the algorithm first proposed by Miller [5] and it incorporates many physically useful features. In particular, the force field determination ignores all angular harmonics of the density distribution higher than a certain order, usually the tenth harmonic. This implies that if the density distribution has more than ninefold symmetry, then the force field will be that of a perfectly axially symmetric distribution. Combined with quiet start procedures, this permits a modest reduction in the number of particles needed to simulate a cold smooth disc. Unfortunately, we cannot exploit this advantage in the case of warm discs since larger numbers of particles are required for other reasons. The usual worry with such a filtering procedure is that physically real fine detail is suppressed in the models. Disc galaxies have a smooth density distribution in azimuth which is very adequately represented by a few low order harmonics, whereas the radial density profile is steep and may oscillate rapidly, e.g., bisymmetric spiral arms are often wound quite tightly. Thus the code is ideally matched to the physical situation to be simulated.

2. The Galaxy Code

The galaxy code resembles that proposed by Miller [5]. We shall emphasize those developments of his algorithm introduced here. The reader is referred to Miller's paper for a fuller description.

The code employs a 2–D polar coordinate grid for calculation of the force field at each time step. The grid points are positioned on $\mathbf{N}_a$ radial lines having an angular separation $\alpha = 2\pi/\mathbf{N}_a$. The radial spacing is logarithmic, grid points having radii given by $Le^{\alpha u}$, where $\mathbf{u}$ is an integer $0 \leqslant \mathbf{u} \leqslant \mathbf{N}_r - 1$, and $\mathbf{L}$ a convenient length unit.

The force field is determined from the mass distribution by a method equivalent to direct summation over all pairs of grid points. Fourier analysis in azimuth reduces the work required to manageable proportions. Unlike Miller, we have preferred to form the radial and tangential components of the force field separately, rather than to solve for the potential which then has to be differenced to yield the force components. This stratagem leads to superior results from less work: first, the errors of difference approximations to a gradient are eliminated and second, resolution is improved by a factor of two. This is because first central differences (as are commonly used) give a gradient smoothed over two cells. The additional cost is one extra summation and one extra Fourier synthesis, whereas to achieve comparable resolution from a potential determination would require four times the number of grid points.

All angular harmonics from 0 to $\mathbf{N}_a/2$ could be included in the evaluation of the force field, although we do not expect any physically meaningful signal in the higher harmonics. Considerable savings in computer time and storage can be made if the higher harmonics are discarded, and for most of this work we have retained only the 0–9 Fourier harmonics for determination of the force field for all grid sizes used. As discussed in the Introduction, the full resolution in radius is desirable on physical grounds and has been retained. The combination of a grid with high frequency

filtering is perhaps rather inelegant; its main justification is that it is a logical development of the code which works well.

The mass of each particle is distributed over the four nearest grid points using area weighting and bilinear interpolation between grid points is used to evaluate the acceleration components for each particle. In contrast to Cartesian grids, this procedure does not ensure linear momentum conservation on a polar grid. There is even a small force, directed towards the grid centre, exerted by each particle on itself. This arises because the directions of the radial (and tangential) force components are not parallel on adjacent grid lines. The self-force varies with position in the grid cell but is easily calculated for each star and is subtracted out at each step.

The motion of the particles was integrated using the time-centred equations of motion for this coordinate system proposed by Buneman [22]. Small denominators occur when particles move radially inward at speeds approaching α^{-1} units in **u** per time step. Accordingly the time step is set to be short enough that a particle falling freely from the edge of the grid will just fail to reach this speed. Particles crossing the outer boundary of the grid are discarded, while those entering the central hole cross it on rectilinear paths and are repositioned on the grid with the same energy one calculation cycle later.

Total energy and angular momentum are conserved to better than 0.1% until stars begin to spill over the outer boundary of the grid (after perhaps 500 time steps). During this period the centre of mass of each model remains within 10^{-3}**L** of the grid centre.

The procedure for measuring the growth of modes is identical to that described by Zang and Hohl [6]. The potential energy inner product

$$\int r\,dr \int d\theta\, \Sigma(r, \theta, t)\, S(r) \cos|m\theta + \psi(r) - \Theta| \tag{1}$$

gives the amplitude of an **m**-fold symmetric mode, when the phase Θ is chosen to maximise the integral. Here, Σ is the surface density of particles in the simulation and **S** and ψ are known functions which describe the shape of the mode potential. An alternative estimate can be made from the potential in the model, in place of Σ, in which case the functions **S** and ψ should then be those appropriate to the mode density. We have obtained very consistent measurements of mode growth in all models from both methods.

3. Cold Disc Simulations

(a) *Theoretical Background*

One of the cold discs studied by Kalnajs and Toomre (unpublished) has the surface density Σ distribution

$$\Sigma(r) = \frac{M}{2\pi a^2}\left(1 + \frac{r^2}{a^2}\right)^{-3/2}, \tag{2}$$

where **r** is the distance from the centre, **a** is a scale length, and **M** is the total mass of the disc. When the gravitational potential at a distance **D** from a unit mass has the softened form

$$\phi(D) = -G(D^2 + d^2)^{-1/2}, \tag{3}$$

where **d** is denoted as the softening length, the potential Φ in the plane of this disc is

$$\Phi(r) = -GM(c^2 + r^2)^{-1/2}, \tag{4}$$

where $\mathbf{c} = \mathbf{a} + \mathbf{d}$ [13].

The initial stellar velocities are exactly tangential and balance the central attraction. If **d** is no smaller than **a/e**, the disc is everywhere stable to local axisymmetric perturbations even when all stars follow exactly circular orbits [17].

There remain many global, nonaxisymmetric unstable modes for this cold disc which have been determined by Kalnajs and Toomre. (Their method is given in [14].) The most rapidly growing mode, denoted mode A, is an open, trailing, bisymmetric spiral mode of the form

$$A(r, \theta, t) = e^{st}\, S(r) \cos|2\theta - 2\Omega_p t + \psi(r)|, \tag{5}$$

where **s** is the growth rate, Ω_p the pattern speed, and **S** and ψ are functions of radius which determine the shape of the mode. Kalnajs and Toomre kindly sent us tabulated values of these functions for the perturbation density and potential of mode A so that we could measure **s** and Ω_p from computer simulations. Their predicted values are $\mathbf{s} = 0.158$ and $\Omega_p = 0.270$ in units, where **M**, **G**, and **a** are all unity, when $\mathbf{d} = \mathbf{a/e}$.

As the disc is infinite in extent, we abruptly truncated the surface density at $\mathbf{r} = 5\mathbf{a}$, discarding in the process 20% of the mass. The cut-off seems to be sufficiently far out to be unimportant for mode A since the function $\mathbf{S(r)}$ is very small outside $\mathbf{r} = 3\mathbf{a}$. The inner boundary of the grid (see Section 2) lies at $\mathbf{r} = 0.1\mathbf{a}$ so 0.5% of the mass is excluded at the centre.

(b) *Results from Noisy Start Models*

The conventional procedure to set up such a model is to choose radial coordinates at random from the distribution which yields the correct surface density profile and azimuthal coordinates from a uniform distribution. Tangential velocity components are perhaps set so as to exactly balance the grid calculated radial force at the start, radial components being set to zero.

Figure 1 shows a typical result from a model constructed in this manner. After fluctuating growth at first, the mode amplitude exponentiates at a steady rate for two **e** folding periods before levelling off to some limiting value. The later stages are presumably dominated by nonlinear effects since the peak final amplitude of the mode exceeds the local mean density.

Both the pattern speed and growth rate are obtained by a least squares fit to the data points in the indicated ranges and the slopes and possible internal errors are

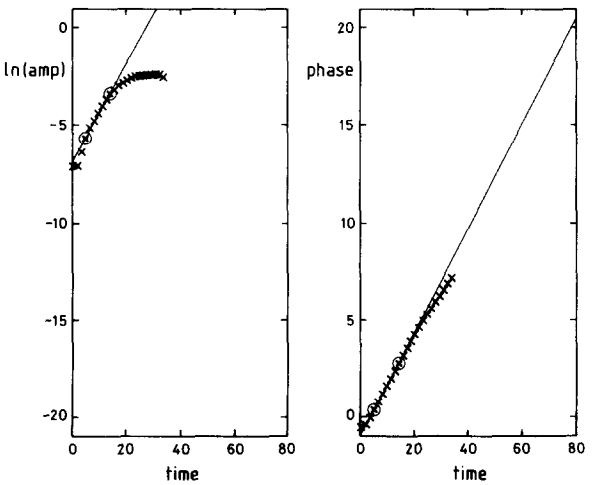

FIG. 1. Measurements of mode A in the cold disc when the initial coordinates of all 20,000 particles were generated in a random manner and the grid has 62×96 cells. The straight lines are least-squares fits to the points in the indicated ranges giving a growth rate of 0.251 ± 0.004 and a pattern speed of 0.268.

noted. The fits are very good; the pattern speed lies close to the predicted value, but the growth rate is too large by 50%.

This result scarcely changes when grid size and time step are varied, but the growth rate alters dramatically as the number of particles is increased as shown in Fig. 2. Although the decline is not always monotonic, there is a tendency for the growth rate to slowly approach the theoretical value as the number of particles is increased, but even 160,000 particles gives an error of ~15%.

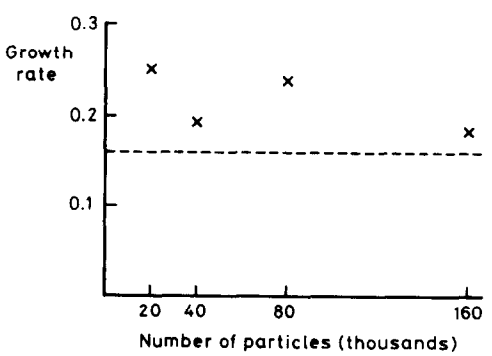

FIG. 2. Growth rates measured from models without quiet starts. The horizontal line shows the value predicted from linear theory. Notice how slowly the results converge to the linear estimate as the number of particles is increased.

This behaviour is symptomatic of noise, the relative importance of which should decrease as the square root of the number of particles. The random distribution of particles introduces a whole spectrum of evolving transients, etc., which hinders isolation of the mode. Indeed, Toomre and Kalnajs (in preparation) are able to predict the error caused by the noise. They find that anomalously high growth rates should be "observed" for most random choices of coordinates. A comparison between their calculations and the noisy models described here is in hand.

(c) *Quiet Start Procedure and Results*

Noise can easily be reduced in these cold discs. For a quiet start, particles are spaced evenly around rings, whose radii correspond to equal increments in mass of the desired disc.[1] This procedure closely corresponds to that described by Byers and Grewal [8], but we have found that a small random displacement in the azimuthal coordinate at the start gives slightly better results than forcing growth to begin from round-off error.

In addition the initial tangential velocities $\mathbf{V}_c$ may be set from the theoretical rotation curve

$$V_c^2 = GMr^2(c^2 + r^2)^{-3/2}. \tag{6}$$

The radial force determined from the calculation grid differs very slightly from the theoretical force (rms error 3.4%), the discrepancy being mainly a result of the absence of mass in the central hole and outside the outer cut-off. This small discrepancy can also be eliminated by adding a small correcting force to the grid determined force at each calculation cycle; the unchanging correction being the difference between the theoretical and mesh-calculated forces at the start.

The result from a model constructed in this way, having 10,000 particles, is shown in Fig. 3a. Ten stars were placed on each ring, spaced evenly in azimuth except for an additional random displacement of up to $2\pi 10^{-4}$ radians, i.e., 0.1% of their mean angular separation. In addition, each ring was rotated through a random angle in order that the configuration did not resemble a 10 spoked wheel. Mode A in this model was observed to grow linearly for six **e** folding times at a rate given in Table I, which is within 2% of the theoretically predicted value. Notice also that the initial amplitude of the mode is three orders of magnitude lower than in Fig. 1.

It might, correctly, be argued that 10 particles per ring are adequate only because angular harmonics higher than nine are filtered out during the field determination. When 20 harmonics are included for the same initial particle distribution, the result shown in Fig. 3b is obtained. Not surprisingly, the model develops a strong tenfold symmetric spiral shaped instability at an early stage. The large amplitude of this instability causes considerable random motion and some rearrangement of the radial distribution of mass, which clearly interferes with the growth of mode A.

[1] Some previous experiments [5] with other cold discs were also started in this way. Miller reports these models to be stable and suggests that the unstable equilibrium is preserved by his integer representation of particle coordinates.

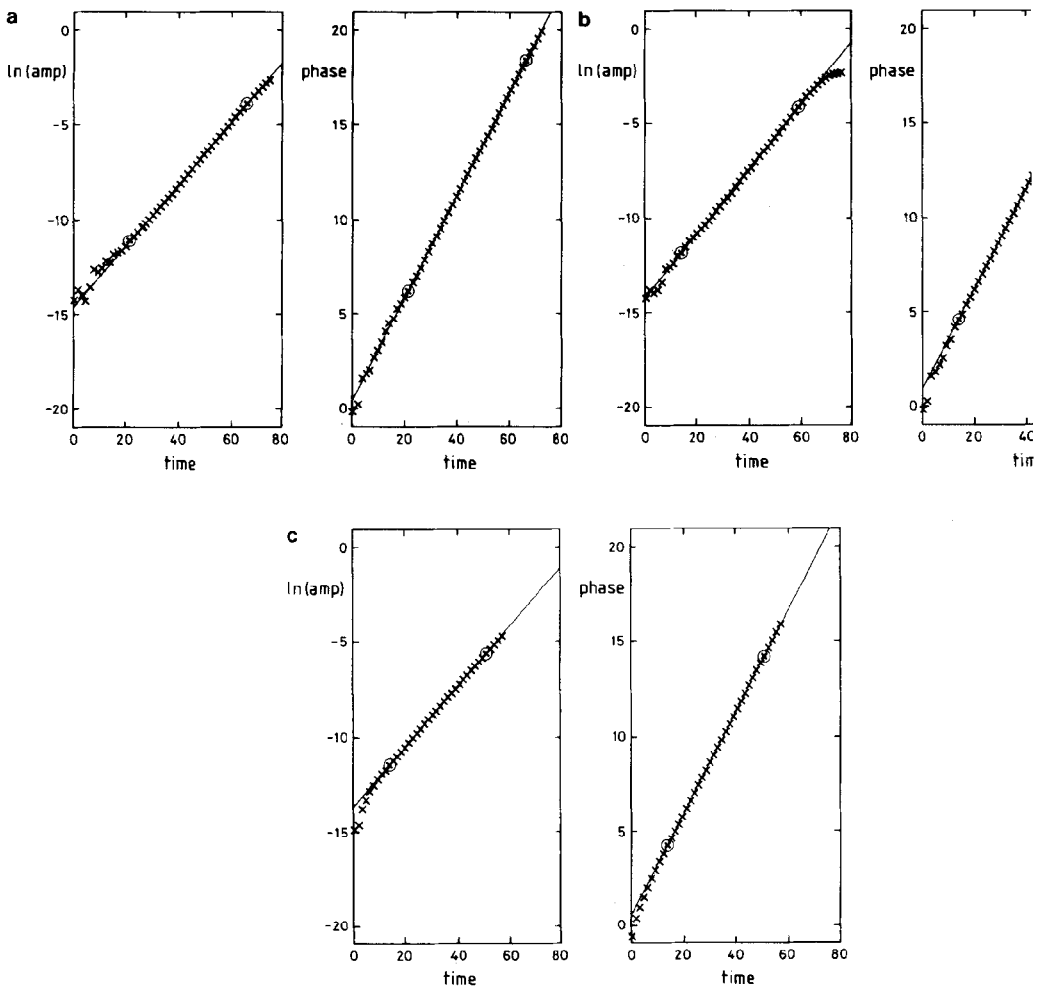

FIG. 3. Measurements of mode A in three cold disc simulations having quiet starts. The differences between the models are described in the text and the slopes of the linear fits are listed in Table I.

Figure 3c shows the result from a further model having eight times the number of rings of particles, but still with 10 to each ring, and in which again the first 20 Fourier harmonics contributed to the force determination. In this case, it is clear than any tenfold symmetric pattern does not significantly affect the growth of mode A. This is because it does not reach sufficient amplitude to interfere with other modes.

It is worth understanding why simply increasing the number of rings of particles should reduce the amplitude of the 10-armed mode. Since each ring is rotated through a random angle, the phases of the 10th harmonic of each ring are distributed more

TABLE I

Mode Frequencies Measured from Simulations of a Cold Stellar Disc Employing Quiet Start Procedures

N	Grid	Fourier harmonics	s		Ω_p	
2	63 × 96	0–9	0.186	0.179	0.295	0.295
5	63 × 96	0–9	0.143	0.145	0.279	0.279
10	63 × 96	0–9	0.161	0.160	0.271	0.271
20	63 × 96	0–9	0.160	0.160	0.269	0.269
2	63 × 96	0–19	0.125	0.131	0.269	0.268
5	63 × 96	0–19	0.176	0.175	0.232	0.232
10	63 × 96	0–19	0.170	0.170	0.266	0.266
20	63 × 96	0–19	0.177	0.176	0.260	0.260
40	63 × 96	0–19	0.157	0.157	0.270	0.270
80	63 × 96	0–19	0.157	0.157	0.266	0.266
10	25 × 36	0–9	0.153	0.153	0.264	0.264
10	63 × 96	0–9	0.161	0.153	0.271	0.270

Note. N gives the number of particles in thousands.

smoothly when more rings are used. This causes the amplitude of the 10th harmonic to be much lower at the start. Mode A, the fastest growing mode, now has enough time to outgrow all others without interference even though the weaker 10-armed pattern had a head start.

The results from these experiments are summarised in Table I, where two estimates of $\mathbf{s}$ and Ω_p are given for each run. These are obtained from the two alternative methods of measurement given in Section 2. Other results are included in Table I from experiments having differing numbers of particles which show a slow but continuing convergence to the linear theory results as the number of particles is increased.

The last two results in this table are from models which differed in other respects. The first of these employed a coarser grid which yielded somewhat slower growth. Wherever the spacing between grid points approaches, or exceeds, the nominal softening length $\mathbf{d}$, as in the outer parts of this coarse grid, additional softening is inevitable [7]. The results and discussion of the next section indicate that additional softening is the likely cause of the reduced growth rate in this model.

The final result is from a model in which initial velocities balance the uncorrected grid determined radial force. The good results obtained demonstrate that the correcting forces added in the previous models were not crucial, and that in other more complicated models, where the theoretical force may be difficult to calculate, simple velocity balance is quite satisfactory for assignment of initial velocities in a cold disc.

4. Warm Disc Simulations

(a) *Theoretical Background*

The only complete modal analysis of warm stellar discs available in the literature (Kalnajs [15]) is that of a family of uniformly rotating discs. All these discs have the surface density distribution

$$\Sigma(r) = \begin{cases} \dfrac{3M}{2\pi R^2}\left(1 - \dfrac{r^2}{R^2}\right)^{1/2}, & r < R, \\ 0, & r > R, \end{cases} \tag{7}$$

which gives rise to a simple harmonic potential well in the region $r < R$; the characteristic angular frequency Ω_0 being given by

$$\Omega_0 = \frac{3\pi GM}{4R^3}. \tag{8}$$

A convenient choice of units are those where $\mathbf{R} = 1$, $\mathbf{M} = 2\pi/3$, and $\mathbf{G} = 2/\pi^2$; causing $\Omega_0 = 1$ and $\Sigma(0) = 1$.

The distribution function[2]

$$\begin{aligned} F(E, J)\, dE dJ &= [\tfrac{1}{2}(1 - \Omega^2)^{1/2}]^{-1}[1 - \Omega^2 - 2(E - \Omega J)]^{-1/2}\, dE dJ, \\ &\qquad 2(E - \Omega J) < 1 - \Omega^2, \\ &= 0, \qquad 2(E - \Omega J) > 1 - \Omega^2, \end{aligned} \tag{9}$$

is a self-consistent solution of both Vlasov's and Poisson's equations. In this, **E** is the energy per unit mass, kinetic plus potential with the zero of potential at the centre of the disc, and **J** is the angular momentum per unit mass. Further restrictions on **E** and **J** are $|J| \leqslant E \leqslant 1$.

Ω characterises the mean rate of rotation of the disc. When $\Omega = 1$ all stars move on exactly circular orbits and the disc is cold. When $\Omega = 0$, the disc is supported purely by random motion, while for intermediate values, some random motion makes up for incomplete rotational support.

Kalnajs has shown that the normal modes have the functional forms of associated Legendre functions and he gives the mode equation from which the frequencies of each mode can be determined. No member of the family is stable to all modes. However, all axisymmetric modes become stable as Ω is reduced below 0.816, as do most of the higher order nonaxisymmetric modes.

[2] Distribution functions conventionally define the density of stars in position-velocity space. The density in energy-angular momentum space given here will be more useful later.

TABLE II

Linear Theory Predictions for the Frequencies of the Four Lowest Order Unstable Modes of the $\Omega = 0.8$ Uniformly Rotating Disc

Mode	Growth rate	Pattern speed
(2, 2)	0.553	0.483
(3, 3)	0.648	0.641
(4, 4)	0.640	0.718
(4, 2)	0.345	1.124

(b) *Computational Implementation*

Hohl [16] has described simulations of four of these discs, having $\Omega = 0.8$, 0.6, 0.4, and 0. He found that the first two of these models formed bars while the second two scarcely evolved. Comparing this with Kalnajs' analysis, which predicts that the (2, 2) mode should be stable for $\Omega < 0.507$, Hohl concluded that his experiments were in agreement. However, he did not attempt to study the growth of individual modes in his simulations. We have chosen to simulate discs having $\Omega = 0.8$, for which the growth rates and pattern speeds of several of the most rapidly growing modes are given in Table II.

The disc, being finite, can be accommodated on the computational grid with only a central cut-out. Less than 0.1% of the mass is excluded at the centre if the central hole has a radius $0.025R$. Nevertheless, substantial differences arise between the theoretical radial force and that produced by the code (see Fig. 4). This discrepancy is almost entirely because of the use of softened gravity in the simulation. Since both the distribution function and the normal modes given by Kalnajs are for the theoretical radial force, it is *vital* that additional forces be added throughout the calculation to correct for this discrepancy as described in Section 3c. Even when this is done, softening depresses the growth rates of unstable modes quite substantially. In fact, strictly speaking the functional forms of the normal modes are changed because the softened perturbation potential will force a slightly different density response. Hopefully, if the softening length is short enough, this will not matter too much.

The reader is reminded that softening is necessary in order to ensure that the simulation mimics a collisionless fluid whilst employing managable numbers of particles. Where many particles are located in each cell, grid softening [7] is adequate for this. In a polar grid, however, cell sizes vary with radius and, unless the particle density is also sharply peaked towards the centre, this region may easily become collision dominated. This problem is readily overcome if we increase the softening by modifying the interparticle force in the manner given by Eq. (3)

comparable to, or exceed **d**. This is a disadvantage inherent in the polar grid; either some additional softening has to be tolerated in the outer parts, or the grid must be

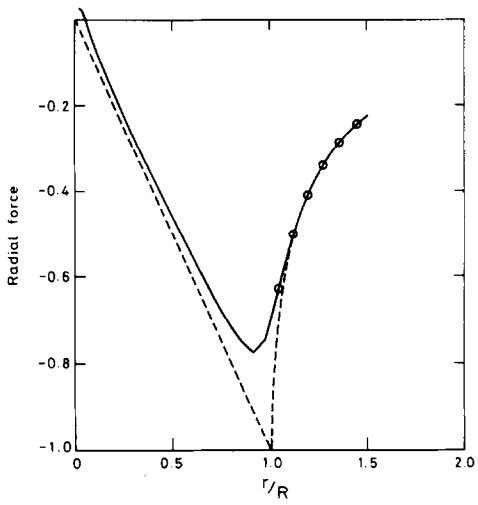

FIG. 4. The grid determined radial force (full drawn curve) and the theoretical force (dashed curve) for the uniformly rotating disc. The discrepancy between the two curves arises principally from the use of softened gravity in the computer model. For this plot $\mathbf{d} = 0.05\mathbf{R}$ and the grid has 63×96 points. The central hole has a radius of $0.025\mathbf{R}$. The circles indicate the measured values at all grid points for which $\mathbf{r} > \mathbf{R}$ and demonstrate the coarseness of the grid in this region.

made fine enough for all dimensions never to approach **d**. Small values of **d** render the second alternative prohibitively expensive.

(c) *Quiet Start Procedure*

Four initial coordinates (i.e., position and velocity components) have to be chosen from the desired distributions for each particle in a warm disc. Models in which these were selected in a random manner yielded discrepancies of up to 25% in the pattern speeds and growth rates which varied between 0.32 and 0.61 for the (2, 2) mode as the numerical parameters were changed. Obviously quiet starts are also necessary for warm discs.

It is insufficient to eliminate noise in the position coordinates alone since random velocities will ensure that the low noise configuration is only momentary. An ideal quiet start will require a smooth distribution in all four variables. Gitomer [10, 11] and Sternlieb [12] use smooth distributions in position space and further reduce noise at the start by applying a correction to the initial randomly generated velocities in order to ensure that the first and second moments of the velocity distribution, when averaged over some volume, are equal to those intended in each component. We have not followed their procedure, partly because the velocity distributions are not Gaussian and are therefore unsuited to this treatment, but mainly because the principle first used by Byers and Grewal [8] can be extended in a more logical manner as follows:

All stars having the same values of **E** and **J** lie in an annular ring whose boundaries are determined by the potential well of the disc. The position of a star is uniquely specified only by the choice of two further variables, the radial and azimuthal phases. The radial phase, together with **E** and **J**, also fixes both velocity components, so several stars having identical **E**, **J**, and radial phase but evenly spaced in azimuthal phase, will remain evenly spaced for as long as the potential remains axially symmetric. This ring of stars will advance in radial phase with time, and will therefore oscillate in radius giving rise to axisymmetric fluctuations in density. These may be reduced by spacing several such rings of stars evenly in radial phase. Obviously, as the number of rings is increased the smaller the axisymmetric fluctuations in density become. Ultimately, we could envisage the separation of successive rings to be equal to the change in radial phase in one time step in the model, which would result in a precisely stationary mass distribution on that orbit. Unfortunately this would require an impractical number of particles: in the present models, with 10 stars on each ring and 50π rings required to suppress axisymmetric fluctuations completely, few such orbits could be represented with $\sim 10^5$ particles. We tried models having 40 rings of 10 stars evenly spaced in radial phase on each of 200 orbits chosen to represent the distribution function. However, different methods of choosing the **E**, **J** pairs from the distribution function produced growth rates which varied by 15% from model to model. These variations appeared to result from there being too few orbits to represent the distribution function adequately.

The best results were obtained when we abandoned the attempt to populate the radial phase smoothly. For every **E**, **J** pair we placed 10 stars almost evenly around the ring defined by one randomly chosen radial phase. This appeared to be the best compromise between creating a stationary density distribution and retaining many orbits to represent the distribution function adequately. It ensures that little noise is present in the lowest angular harmonics while relying on a large number of particles to keep axisymmetric oscillations at low amplitude. Axial symmetry is more important because all unstable modes of the models to be investigated are nonaxisymmetric. Fortunately, this is generally true for most galaxy models of interest. Axisymmetric stability is well understood [17, 23] and relatively easy to achieve. However, radial fluctuations may still be troublesome if the instabilities have the shape of tightly wound spirals.

The chosen **E**, **J** pairs should also be distributed smoothly. One possible method for this is to integrate **F** over **E** and **J** to determine the fraction of mass having **J** less than a certain value. Equal steps in this mass fraction define **J**; **E** values are chosen in equal increments of mass fraction along the cut at this **J**. Several equivalent methods, which led to different but smoothly distributed choices of **E**, **J** values gave growth rates consistent to 5% while random choices from the distribution function led to variations about twice as large.

(d) *Results for the* (2, 2) *Mode*

The values of **s** and Ω_p measured from four simulations having differing softening lengths are plotted in Fig. 5a. The uncertainty in each measurement is ~5% (see

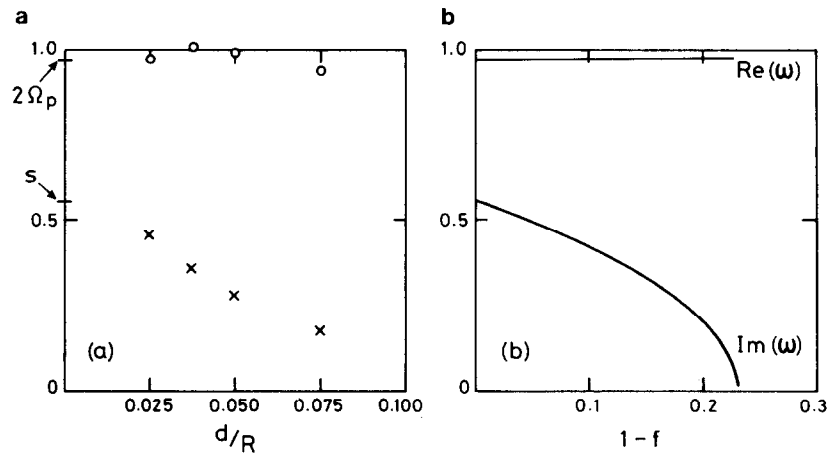

FIG. 5. a The measured growth rates (crosses) and 2 × pattern speeds (circles) from a series of warm disc models having differing softening lengths, **d**. The values marked on the frequency axis are the predictions of linear theory. b The complex roots of the mode equation for the (2, 2) mode in the $\Omega = 0.8$ disc. The **f** is a factor which weakens the disturbance potential without changing its shape.

Section 4(g)). It is clear from this figure that as the softening length is increased the growth rate decreases rapidly while the pattern speed is scarcely affected.

A very loose justification of this behaviour is possible: If the perturbation potential is weakened by a factor $\mathbf{f}(<1)$ without changing its functional form, Kalnajs' equation for normal modes becomes $f\lambda(n, m, \Omega, \omega) = 1$. Figure 5b gives the complex roots of this equation as functions of **f** for the (2, 2) mode in the $\Omega = 0.8$ disc. The growth rate $\mathrm{Im}(\omega)$ decreases rapidly with **f** and the mode becomes stable for $\mathbf{f} < 0.77$. The pattern speed, $\mathrm{Re}(\omega)/m$ with $m = 2$ for the (2, 2) mode, hardly changes with **f**. The softened potential in the disc is equal to the Newtonian potential in a plane parallel to, but offset a distance **d** from the disc, so it is tempting to suppose that $f = \exp(-kd)$. For this to be true, the perturbation density of the mode should have the form of a Bessel function with wave number **k** [13]. Since the (2, 2) mode is very different from a Bessel function and we have also neglected the effect softening must have on the functional forms of the modes, the similarity between Fig. 5a and b is remarkable.

In view of these inadequacies, it seems scarcely worthwhile to try to fit the curve of Fig. 5b to the data in a; a straight line fit should be adequate to extrapolate the measured values to zero softening. Least squares fits give intercepts of 0.573 for the growth rate and 0.508 for the pattern speed which are within 4% and 5%, respectively, of the theoretical values given in Table II.

(e) *Other Modes*

Table III and Fig. 6 give the measurements of the (3, 3), (4, 4), and (4, 2) modes from the same series of models. It is apparent that the model having $\mathbf{d} = 0.075\mathbf{R}$ did

TABLE III

Measured Frequencies of Four Low-Order Modes of the Warm Disc

Grid	N	d/r	(2, 2) Mode		(3, 3) Mode		(4, 4) Mode		(4, 2) Mode	
			s	Ω_p	s	Ω_p	s	Ω_p	s	Ω_p
125 × 192	80	0.025	0.446 0.460	0.483 0.487	0.478 0.492	0.662 0.665	0.439 0.436	0.718 0.718	0.392 0.418	0.480 0.482
94 × 144	80	0.0375	0.354 0.360	0.503 0.501	0.372 0.373	0.647 0.648	0.275 0.279	0.723 0.722	0.322 0.337	0.507 0.501
63 × 96	80	0.050	0.278 0.280	0.496 0.494	0.279 0.283	0.634 0.634	0.165 0.175	0.701 0.697	0.286 0.279	0.496 0.498
42 × 64	80	0.075	0.167 0.181	0.468 0.468	0.287 0.276	0.573 0.594	0.076 0.082	0.533 0.585	0.113 0.152	0.485 0.477

Note. The degree of softening was different in each of the four simulations.

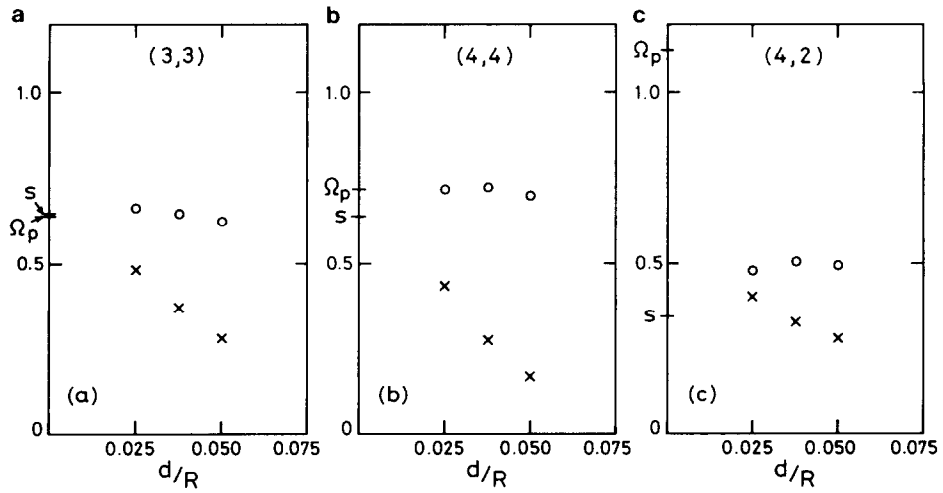

FIG. 6. Measured growth rates (crosses) and pattern speeds (circles) of a the (3, 3) mode, b the (4, 4) mode, and c the (4, 2) mode from the same series of models as for Fig. 5a. Softening has a proportionately larger effect on higher order modes. The (4, 2) mode is badly contaminated by the (2, 2) mode. The values on the frequency axis are the predictions of linear theory.

not produce reliable results for any of these higher modes but the other three models, having less softening, show fairly well-defined trends at least for the (3, 3) and (4, 4) modes. Using values from these three models only, linear fits to the measurements of $\mathbf{s}$ and Ω_p extrapolate to $\mathbf{s} = 0.686$, $\Omega_p = 0.692$ for the (3, 3) mode an $\mathbf{s} = 0.697$, $\Omega_p = 0.742$ for the (4, 4) mode. None of these extrapolated values differs by more than 10% from the theoretical values given in Table II for zero softening.

Comparing Figs. 5a, 6a, and 6b it is evident that the growth rate drops more steeply with increasing softening as we look for higher order modes. This is only to be expected: as the spatial variations in the disturbance density become more rapid the relative importance of smoothing will increase.

The results from the (4, 2) mode are very bad. Not only are the growth rates in some models *higher* than the theoretical values with no softening, but the pattern speeds are all less than half the predicted value. Notice, though, that the results for this mode are very similar to those in Fig. 5a for the (2, 2) mode. Both modes are bisymmetric and differ only in radial profiles and it is apparent that the

tionately more than the (2, 2) mode, as a result of its more rapid spatial variation, and it is likely that the mode is completely stabilised by softening in all these models.

The modes of this disc are untypical, because the interaction potential energy of *any* pair is zero [15]. Thus we should expect that the measurements of the (4, 2) mode would be completely unaffected by the (2, 2) mode. The most likely explanation

of the cross contamination is that softening has changed the forms of the modes sufficiently for their orthogonality properties to be lost.

(f) *Other Forms of Softening*

All results discussed so far have been taken from models in which the nominal softening has the form of Eq. (3). The interparticle force converges only slowly to the

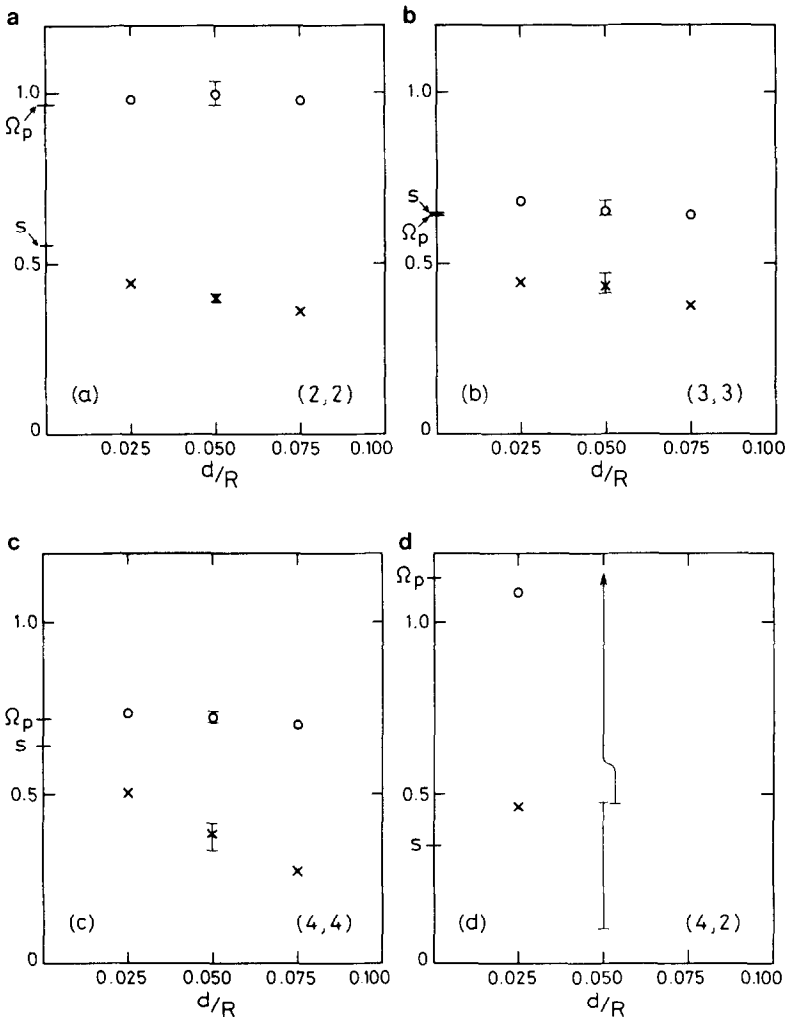

FIG. 7. Measured growth rates (crosses) and pattern speeds (circles) for the four lowest order unstable modes in the $\Omega = 0.8$ disc. Softening in these models followed the eighth power rule of Eq. (10). The error bars show the total range of measurements obtained from six simulations. Notice that growth rates decrease more slowly with softening than in Figs. 4a, 5a and b.

Newtonian law for $\mathbf{D} \gg \mathbf{d}$. A more rapid convergence results if the softened potential has the form

$$\phi^*(D)\, \alpha\, (D^8 + d^8)^{-1/8}. \tag{10}$$

If this is used in the models, the "clouds" associated with each particle merely have a different radial density profile [7].

Figures 7a–d shows that this shorter range softening causes the growth rates to decrease more slowly with increasing **d**. In particular, meaningful results can now be obtained for the (3, 3) and (4, 4) modes when $\mathbf{d} = 0.075\mathbf{R}$. This is a useful feature because for larger values of **d** coarser grids may be used. Extrapolation of these results to zero **d** gives $\mathbf{s} = 0.484$, $\Omega_p = 0.494$ for the (2, 2) mode, $\mathbf{s} = 0.486$, $\Omega_p = 0.700$ for the (3, 3) mode, and $\mathbf{s} = 0.623$, $\Omega_p = 0.752$ for the (4, 4) mode. Unfortunately these are not so close to the theoretical values as for the first form of softening, the worst error is 24% in the growth rate of the (3, 3) mode. Why these extrapolations should agree less well is not clear.

Again the (4, 2) mode is very much worse than the simpler modes, but there is a faint hint from the pattern speed measurements that with this form of softening some signal is detectable when **d** is very small. The growth rate is still much too large, and is presumably grossly contaminated by the (2,2) mode, but it is possible that the mode may not be completely stabilised as patterns speeds of the right magnitude are detected.

(g) *Reliability of the Measurements*

The error bars in Fig. 7 indicate the total range of measured values of **s** and Ω_p obtained from six different simulations. The details of each experiment and the individual results are summarised in Table IV. The largest deviation from the mean value is only 4% for the (2, 2) mode and 8% for the (3, 3) and (4, 4) modes.

Figures 8a–d shows detailed measurements of the (2, 2) mode from three of these models, and a fourth which did not employ a quiet start. Figure 8a merely demonstrates how plausible the incorrect growth rate may appear from a noisy model. Figures 8b and c illustrate the improvement in quality which results from using more particles. Figure 8d shows that the results are largely unchanged when 20 Fourier harmonics contribute to the force determination; in all other warm disc simulations discussed here only 10 angular harmonics are used. As for the cold discs, once large numbers of particles are employed, more harmonics add nothing but noise.

It will be noticed from Tables III and IV that finer grids were used for shorter values of **d**; in fact grid sizes were changed in strict proportion to **d**. In the outer parts of the grids in all these models the cell dimensions exceed **d** and additional grid softening is present [7]. (The cell sizes are about 25% larger than **d** near the outer edge of the unperturbed disc, which is at a radius of 40 grid units.) The extra grid softening is significant since growth rates vary by as much as 25% when grid cell sizes are changed while **d** and all other numerical parameters are held fixed. Provided this problem is recognized and grid sizes are adjusted in strict proportion to **d**, the situation is no worse than in a Cartesian grid, where only grid softening is employed.

TABLE IV

Measured Frequencies of the Low Order Modes of the Warm Disc

Grid	N	d/r	(2, 2) Mode		(3, 3) Mode		(4, 4) Mode		(4, 2) Mode	
			s	Ω_p	s	Ω_p	s	Ω_p	s	Ω_p
125 × 192	80	0.025	0.446 0.437	0.487 0.493	0.447 0.439	0.682 0.681	0.505 0.505	0.739 0.732	0.480 0.454	1.087 1.081
63 × 96	20	0.050	0.406 0.395	0.515 0.510	0.425 0.432	0.655 0.655	0.413 0.411	0.708 0.708	0.282 0.328	1.228 0.677
	40		0.402 0.411	0.481 0.481	0.469 0.469	0.647 0.645	0.372 0.392	0.734 0.730	0.401 0.393	0.526 0.518
	80		0.389 0.405	0.482 0.485	0.432 0.439	0.640 0.640	0.360 0.360	0.711 0.712	0.104 0.138	2.353 1.736
	160		0.400 0.402	0.495 0.498	0.428 0.436	0.649 0.648	0.402 0.429	0.724 0.723	0.380 0.393	0.473 0.478
	80[a]		0.410 0.410	0.509 0.507	0.427 0.430	0.649 0.649	0.391 0.383	0.722 0.722	0.477 0.437	0.515 0.511
	80[b]		0.394 0.406	0.496 0.495	0.411 0.421	0.660 0.659	0.332 0.333	0.730 0.728	0.195 0.200	1.234 0.913
42 × 64	80	0.075	0.360 0.364	0.488 0.488	0.377 0.377	0.639 0.639	0.267 0.274	0.702 0.701		
32 × 48	80	0.100	0.071 0.086	0.494 0.496	0.074 0.061	0.599 0.597	0.209 0.198	0.419 0.737		

Note. Unlike the results given in Table III, these models employed the softening expression (10).

[a] New E, J choices.

[b] 20 Fourier harmonics.

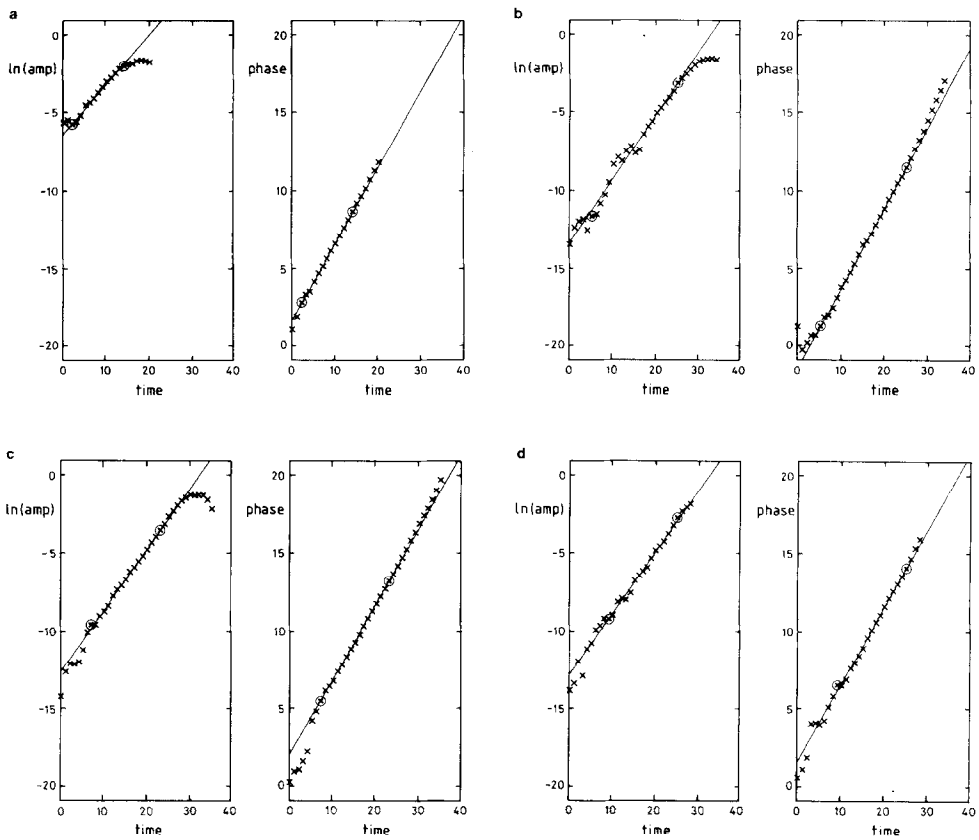

FIG. 8. Measurements of the (2, 2) mode in four warm disc simulations. In (a) the initial coordinates of the 80,000 particles were chosen in a random manner and **d** was 0.05**R**. The slopes of the drawn fits are $\mathbf{s} = 0.323 \pm 0.004$ and $\Omega_p = 0.490 \pm 0.002$. The other models all had quiet starts; for (b) 20,000 particles were used, for (c) 80,000 particles, and for (d) more Fourier harmonics contributed to the force determination. Other details are given in Table IV.

(h) *Nonlinear Behaviour*

Figure 8 also demonstrates that linear growth can be maintained in the models for nearly eight **e** folding periods before nonlinear effects become important. As for the cold discs, these occur as the perturbation amplitude approaches the mean density over a significant fraction of the disc.

The limiting amplitude of the (2, 2) mode varied by no more than 20% from run to run. No systematic changes in the limiting amplitude occurred as the number of particles or Fourier harmonics employed were varied and even noisy start models reached very similar maximum amplitudes. Variations were, however, correlated with the relative strengths of the (2, 2), (3, 3), and (4, 4) modes at the start of nonlinear

behaviour. Notice from Table IV that the growth rates of these three modes are very similar in the models. Therefore their relative amplitudes at late times depend both on the small differences in growth rates and their magnitudes at the start of the run. Even in quiet start discs small variations in the initial amplitude of each mode arise. In models where higher modes were unusually prominent, the growth of the (2, 2) mode tended to cease at a slightly lower amplitude. When higher modes were suppressed, in further models in which only the $m = 0$, 1, and 2 Fourier harmonics contributed to the force field, these variations were eliminated. It is clearly something of a coincidence that the growth rates of the three dominant modes should be so similar in these models.

The (2, 2) mode always triumphs. The final appearance of the model is always bar-like even when the (3, 3) or (4, 4) mode is the first to become visible in the spatial distribution of the particles. The pattern speed of the (2, 2) mode always increases as the limiting amplitude is reached. This is probably the result of mixing of modes; since the pattern speeds of the higher modes are larger, the resulting nonaxisymmetric structure turns at a rate faster than for the pure (2, 2) mode.

5. Summary and Conclusions

The results presented in this paper demonstrate the importance of quiet starts if linear growth of modes in disc galaxies is to be measured from computer simulations. Quiet start procedures are presented for both cold and warm discs.

Uniquely, the polar grid provides the opportunity to vary the number of angular harmonics used to determine the force field. Filtering out all high angular harmonics further suppresses noise in the simulations.

Taking full advantage of this feature, the code is able to reproduce linear growth of modes in a cold disc to a precision of better than 2% when employing ten thousand particles. Without high frequency filtering during the force determination, many more particles are required for the same precision.

More particles are needed for the astronomically more interesting warm disc simulations, because the population of particles has to represent a distribution of velocities in addition to a radial density profile. Despite the further complication introduced by softening, growth rate and pattern speeds within 10% of the theoretical values were found for the three lowest order modes in a uniformly rotating disc.

Previous work [18] had shown that the growth of instabilities in discs can be totally suppressed by softening and it is therefore important that softening should be as small as possible. In this paper, the relative importance of softening is shown to increase steadily with the order of the mode. Obviously, shorter softening lengths, and therefore finer grids, are necessary as one wishes to resolve finer details. The grid sizes used in this paper seem adequate to resolve only global instabilities.

In all models, steady linear growth is observed over many **e** folding periods and nonlinear behaviour sets in only when the density contrast produced by the fastest growing mode is of order unity. Although no analytic treatment is available which

could predict the amplitude at which nonlinear behaviour becomes important, it seems reasonable that it should occur at this level. It is also reassuring that the maximum amplitude should be so similar in the various models shown in Fig. 8, including that of having a noisy start.

This conclusion is important, since many models have been described in the literature ([18] and references therein) in which the starting configuration was chosen in a random manner. Most results from these models concern the nonlinear behaviour of large amplitude stellar bars which should not be unduly affected by noise in the initial configuration. Other nonlinear effects to be reported are associated with variable spiral structure in apparently globally stable discs [19–21]. The extent to which these features are influenced by fluctuations in the distributions of small numbers of particles is less clear.

This work has demonstrated that a great deal of care is necessary to ensure that a computer simulation employing a few tens of thousands of stars properly manifests the instabilities of a smooth disc. It does *not* automatically follow that, were a smooth disc stable to small preturbations to be simulated, the model will exhibit no growth.

Finally, it should be recognized that a smooth disc is a theoretician's abstraction. Most real galaxies contain lumps and asymmetries in the distribution of several of their constituent components. Thus noisy computer simulations may, in this sense, be closer to reality than smooth discs. Nevertheless, it remains true that our understanding of the complex problems of galaxy dynamics will be helped if the effects of noise are separated from modal instabilities.

ACKNOWLEDGMENTS

The author would like to thank Professor A. Toomre and Dr. A. Kalnajs for originally suggesting that we try to reproduce their mode analyses and for many thoughtful comments at all stages of the work. The computations were performed as background jobs on the SERC "Starlink" VAX and their cooperation is appreciated.

REFERENCES

1. R. W. HOCKNEY, *Methods Comput. Phys.* **9** (1970), 135.
2. R. W. HOCKNEY AND J. W. EASTWOOD, "Computer Simulation using Particles," McGraw–Hill, New York, 1981.
3. F. HOHL, NASA Tech. Rep. No. R-343 (1970).
4. F. HOHL, *Astrophys. J.* **184** (1973), 353.
5. R. H. MILLER, *J. Comput. Phys.* **21** (1976), 400.
6. T. A. ZANG AND F. HOHL, *Astrophys. J.* **226** (1978), 521.
7. A. B. LANGDON AND C. K. BIRDSALL, *Phys. Fluids* **13** (1970), 2115.
8. J. A. BYERS AND M. GREWAL, *Phys. Fluids* **13** (1970), 1819.
9. R. L. MORSE AND C. W. NIELSON, *Phys. Fluids* **14** (1971), 830.
10. S. J. GITOMER, *Phys. Fluids* **14** (1971), 1591.

11. S. J. GITOMER, *Phys. Fluids* **14** (1971), 2234.
12. A. STERNLIEB, *J. Comput. Phys.* **25** (1977), 118.
13. A. TOOMRE, *Astrophys. J.* **138** (1963), 385.
14. A. J. KALNAJS, *Astrophys. J.* **212** (1977), 637.
15. A. J. KALNAJS, *Astrophys. J.* **175** (1972), 63.
16. F. HOHL, *J. Comput. Phys.* **9** (1972), 10.
17. A. TOOMRE, *Astrophys. J.* **139** (1964), 1217.
18. J. A. SELLWOOD, *Astron. Astrophys.* **99** (1981), 362.
19. R. W. HOCKNEY AND D. R. K. BROWNRIGG, *Mon. Not. Roy. Astron. Soc.* **167** (1974), 351.
20. R. A. JAMES AND J. A. SELLWOOD, *Mon. Not. Roy. Astron. Soc.* **182** (1978), 331.
21. R. H. BERMAN, D. R. K. BROWNRIGG, AND R. W. HOCKNEY, *Mon. Not. Roy Astron. Soc.* **185** (1978), 861.
22. O. BUNEMAN, *J. Comput. Phys.* **1** (1967), 517.
23. R. H. MILLER, *Astrophys. J.* **226** (1978), 81.